Composite microcapsules with enhanced mechanical stability and reduced active ingredient leakage

Long, Yue; Song, Kai; York, D; Zhang, Zhibing; Preece, Jon

DOI:
10.1016/j.partic.2015.09.003

Document Version
Peer reviewed version

Citation for published version (Harvard):
Long, Y, Song, K, York, D, Zhang, Z & Preece, J 2015, 'Composite microcapsules with enhanced mechanical stability and reduced active ingredient leakage', *Particuology*. https://doi.org/10.1016/j.partic.2015.09.003

Composite microcapsules with enhanced mechanical stability and reduced active ingredient leakage

Yue Long[a,b,*], Kai Song[b], David York[c], Zhibing Zhang[d], Jon A. Preece[a,*]

[a]School of Chemistry, University of Birmingham, Edgbaston, Birmingham, B15 2TT, UK

[b]Laboratory of Bio-Inspired Smart Interface Science, Technical Institute of Physics and Chemistry, Chinese Academy of Sciences, Beijing 100190, China

[c]Institute of Particle Science & Engineering, School of Process, Environmental and Materials Engineering, University of Leeds, Leeds, LS2 9J, UK

[d]School of Chemical Engineering, University of Birmingham, Edgbaston, Birmingham, B15 2TT, UK

*Corresponding author. Tel: +86 10 82617303 or +44 (0)121 414 3528; E-mail: longyue@mail.ipc.ac.cn (Y. Long); j.a.preece@bham.ac.uk (J.A. Preece)

Abstract A calcium shellac (CS) matrix was used to encapsulate polymeric melamine formaldehyde microcapsules (A) or $CaCO_3$ nanoparticles-stabilized microcapsules (B), both of which encapsulated an oil-based active ingredient, producing A-CS or B-CS composite microcapsules. The mechanical properties and oil release profiles of the composite microcapsules were evaluated. The composite microcapsules showed enhanced mechanical stability and reduced leakage of the active ingredient by one order of magnitude.

Keywords: Composite, Microcapsule, Calcium shellac, Mechanical property, Control release, Perfume oil

1. Introduction

Microencapsulation is a powerful technology with a wide range of applications that can enhance the stability of active ingredients, aid conversion of liquids to free flowing powders, target the encapsulated compound to specific sites, and provide prolonged and controlled release of active ingredients (Yow & Routh, 2006). Sustained release microcapsule formulations often rely on diffusion of active ingredients from the core through a permeable outer coating or wall to the desired site (Sukhorukov, Fery, Brumen, & Möhwald, 2004). However, permeability of the microcapsule wall can also lead to loss of active ingredients from the core during processing and storage, and this is especially problematic for volatile core materials such as perfume oils. This problem has been partially solved using stimuli-responsive materials (Katagiri, Imai, & Koumoto, 2011; Skirtach et al., 2005; Graf et al., 2011; Ke et al., 2011) to form the microcapsule wall. These materials provide an impermeable wall during storage and a permeable wall at end use. However, construction of microcapsules from these materials requires a layer-by-layer deposition method (De Cock et al., 2010), and they are thin-walled and fragile. The low mechanical strength of the wall could greatly affect stability of the microcapsules, and they could rupture during transportation and lead to loss of the active ingredient and increased cost. In addition, these types of capsules can only be produced in small quantities, and are therefore not applicable for industrial application. A system to eliminate or reduce

leakage of the active ingredient from microcapsules and increase the mechanical stability of the wall is required.

An alternative strategy involves taking conventional primary microcapsules with an organic (Long, York, Zhang, & Preece, 2009) or inorganic (Long, Vincent, York, Zhang, & Preece, 2010) wall and encapsulating them in a larger microparticle formed from a biopolymer–shellac cross-linked *via* calcium ions. This outer microparticle can provide good mechanical stiffness and low permeability, and act as a carrier and barrier for the more porous primary microcapsules by protecting them from damage during various processing steps and reducing active ingredient leakage. In principle, the primary microcapsules could be released by dissolution of the biopolymer when needed.

Shellac is a natural polyester containing hydroxyl, carboxylic acid, and ester functionalities (Singh, Upadhye, Mhaskar, & Dev, 1974; Upadhye, Wadia, Mhaskar, & Dev, 1970). Shellac has very low water and acid permeability, and it is frequently used as a coating material in pharmaceutical (Pearnchob, Siepmann, & Bodmeier, 2003; Oehme, Valotis, Krammer, Zimmermann, & Schreier, 2011) and food products (Zhou, Li, Yan, & Xie, 2011; Chauhan, Raju, Singh, & Bawa, 2011). Recently, shellac has been further developed as an encapsulating agent for producing microcapsules (Xue & Zhang, 2009; Leick et al., 2011; Hamad, Stoyanov, & Paunov, 2012, 2013) and tablets (Limmatvapirat et al., 2008), where it enhances water resistance and mechanical strength (Xue & Zhang, 2009; Leick et al., 2011). Because it possesses good resistance to gastric acid and is biodegradable, it is a good candidate for drug carriers in pharmaceutical applications (Ravi, Siddaramaiah, & Kumar, 2008).

In the work reported here, primary microcapsules with walls made from melamine formaldehyde (MF; microcapsule A) (Long et al., 2009) or $CaCO_3$ nanoparticles (microcapsule B) were used to encapsulate perfume oil. These primary microcapsules (A and B) were then encapsulated in calcium shellac (CS) matrix to form composite microcapsules (A-CS) and (B-CS). MF is a widely used as a wall material for microcapsules that are used in many applications, including carbonless copy paper and household products. As an inorganic material, $CaCO_3$ is non-toxic and can be dissolved in weak acid, and has attracted much attention as a wall material. The advantages for such dual wall structure are that firstly, the cost of using shellac as an outer wall to control the mechanical strength of the capsules is relatively low; secondly, with the protection of the shellac matrix, one has more flexibility with respect to the choice of chemistry and stabilizers to minimize chemical interactions with the active species, thus giving the designer more freedom of choice in industrial applications. With the above properties, such microcapsules could be potentially used in household products such as detergents or textiles.

2. Experimental

2.1. Materials

An aqueous solution of shellac ammonium salt (mass fraction (25±0.4)%, pH 7.3±0.3, density 1.04±0.03 kg/L; Emerson Resources, Inc., USA), acetic acid (Sigma–Aldrich, UK), calcium chloride (Sigma–Aldrich), and Tween 80 (Sigma–Aldrich) were obtained and used without further purification. The core oil was a perfume blend with low water solubility that is commonly used in consumer products. An aqueous solution of MF precondensate (mass fraction 70%, formaldehyde:melamine molar ratio 1:5) was obtained from British Industrial Plastics Ltd (Oldbury, UK). An aqueous solution of formaldehyde (mass fraction 37%) was obtained from Sigma-Aldrich, and poly(acrylamide-acrylic acid) sodium salt was purchased from Polymer Sciences, Inc. (USA). Calcium carbonate nanoparticles (average diameter 80 nm) were obtained from Omya (UK) and were used without further purification.

2.2. Preparation of composite microcapsules

2.2.1. Formation of primary microcapsules

An aqueous solution of MF precondensate (2.50 g) and the poly(acrylamide-co-acrylic acid) sodium salt copolymer (0.58 g) in water (70 mL) was stirred with a Rushton turbine (400 rpm, ϕ31 mm, in a standard configuration vessel) for 105 min at room temperature. Before stirring, the pH of the solution was adjusted to 4.3 with acetic acid (1 mol/L), and monitored using a pH meter during stirring. The core oil (9.33 g) was added to the resulting mixture, and the mixture was stirred using a homogenizer (Model L4RT, Silverson Machines Ltd, Chesham, UK) at 2500 rpm for 30 min at 15 °C to form an oil in water emulsion. The resulting emulsion was stirred at 400 rpm in a vessel (ϕ65 mm×65 mm) with a standard Rushton turbine impeller (ϕ31 mm) for 30 min at 15 °C. Then, the temperature was increased to 65 °C and stirring was continued for 6 h. The resulting dispersion of MF microcapsules was then cooled to 25 °C.

To form $CaCO_3$ nanoparticle-stabilized microcapsules (B), the core oil (9.3 g) was added to an aqueous dispersion of $CaCO_3$ nanoparticles (40 mL, mass fraction 10%) and stirred using a homogenizer (Model L4RT, Silverson Machines Ltd) at 2500 rpm for 3 min. This formed an oil in water emulsion stabilized by $CaCO_3$ nanoparticles.

2.2.2. Formation of composite microcapsules

Composite microcapsules of CS containing MF microcapsules (A-CS) or $CaCO_3$ nanoparticle microcapsules (B-CS) were formed as follows. One gram of MF microcapsules (A) or $CaCO_3$ nanoparticle-stabilized microcapsules (B) was dispersed in an aqueous solution of shellac ammonium salt (5 mL). Sunflower oil (200 mL) was added to the resulting dispersion (Step 1, Scheme 1), and the mixture was stirred using a homogenizer (Model L4RT, Silverson Machines Ltd) at 1000 rpm for 30 min. Calcium chloride (0.1 g) was added every minute over 10 min (1 g in total) to the resulting emulsion, and the stirring was maintained for another 2 h until no $CaCl_2$ powder remained; The divalent calcium ions migrated to the oil–water interface and ion exchange occurred with monovalent ammonium ions and the carboxylate anions, resulting in cross-linking of the shellac wall (Step 2, Scheme 1). The resulting composite

capsules (A-CS and B-CS) were isolated from the sunflower oil by filtration and dried using a freeze dryer (EF03, Edwards, Crawley, UK) at −40 to −45 °C for 24 h. The pressure was 4–5 mbar at the end of the drying process.

Scheme 1

CS microparticles were prepared as follows. Sunflower oil (200 mL) was added to the aqueous solution of shellac ammonium salt (5 mL), and the resulting mixture was emulsified using a homogenizer (Model L4RT, Silverson Machines Ltd) at 1000 rpm for 30 min. Calcium chloride (0.1 g) was added every minute over 10 min (1 g in total) to the emulsion, and the stirring was maintained for another 2 h until no $CaCl_2$ powder remained. The resulting microparticles were isolated from the sunflower oil by filtration and freeze dried.

2.3. Characterization of composite microcapsules and CS microparticles

The mean particle size and size distribution of the microcapsules and calcium shellac microparticles in the aqueous dispersions were evaluated by static light-scattering (Mastersizer 2000, Malvern Instruments Ltd, UK).

FIB/SEM (Quanta 3D FEG, FEI Company, USA) was used to examine the inner structures of complex microcapsules and calcium shellac microparticles. Samples were analyzed in high vacuum mode and the operating voltages are shown on the FIB/SEM images.

The mechanical properties of the microcapsules were determined by micromanipulation (Zhang, Saunders, & Thomas, 1999). A glass probe with a diameter of 300 μm mounted on a force transducer (Model 405A, Aurora Scientific Inc., Canada) was positioned perpendicular to the glass slide. The dried microcapsules or calcium shellac microparticles were placed on the glass slide, and observed through side and bottom-view cameras. A single microcapsule or calcium shellac microparticle was compressed by the glass probe travelling at 2 μm/s. The voltage output generated by the force transducer because of compression of the microcapsules or calcium shellac microparticles was recorded through a data acquisition card in a personal computer. From the sensitivity of the transducer, the voltage was converted to force and used to determine the rupture force of the microcapsules or calcium shellac microparticles.

To determine oil encapsulation efficiency and leakage rate of the microcapsules, a Trace 2000 series gas chromatogram with a flame ionization detector and ZB5 Inferno column (30 m×0.32 mm) was used. Analysis was performed using a Dionex Chromeleon Workstation. The injection volume of each sample was 1 μL. The injection port temperature was 250 °C. The temperature ramp for the column was increased by 10 °C/s from 50–300 °C, and held at 300 °C for 35 min. The detection temperature was 300 °C. Helium was used as the carrier gas.

To the resulting aqueous dispersion of microcapsules, hexane was added (30 mL), which was stirred for 10 min. A hexane aliquot (1 μL) was then removed and analyzed by gas chromatography to determine the amount of oil. Further aliquots (1 μL each) were removed at various time intervals between 1 to 20 d. Before each sample was removed, the dispersion was stirred for 10 min to ensure oil transfer to the hexane layer.

3. Results and discussion

3.1. Size and morphology

The mean particle size and size distribution of the primary and composite microcapsules are shown in Fig. 1. The primary microcapsules A and B had average diameters of 13.1 and 13.8 μm, respectively. After re-encapsulated in the CS shell, the average diameters of A-CS and B-CS increased to 83.0 and 84.0 μm, respectively. By comparison, the average diameter of a CS microparticle was 42.6 μm. It is worth noting that both CS and the composite A-CS and B-CS presented bimodal distribution curves. The first peak in these curves was small and might be caused by the formation of small droplets during emulsification. These droplets would then solidify to form CS microparticles in the shell formation step. For the microcapsules made from MF, the small peak was caused by MF polymer particle formation during the polymerization step.

Fig. 1

Optical and electron microscopy were used to examine the structures and morphologies of the composite microcapsules A-CS and B-CS and the microparticle CS (Fig. 2). A comparison of the optical microscopy images (Fig. 2(a), (c), and (e)) showed that microcapsules A and B were encapsulated in the irregularly shaped CS matrix, and had rough surfaces (Fig. 2(b) and (d)). FIB/SEM was used to examine the inner structure of the B-CS composite microcapsules (Fig. 2(d)) and CS microparticles (Fig. 2(f)). In agreement with an earlier report (Xue & Zhang, 2009; Hamad et al., 2012), SEM imaging revealed that the CS microparticles had a solid interior (Fig. 2(f)). By contrast, the B-CS composite microcapsules contained voids (hollows), and the core oil was leaking from the bottom edge of the hollow (Fig. 2(d)). The hollow in the image (Fig. 2(d)) had a diameter of approximately 30 μm, which is within to the diameter range of the B microcapsules (4–37 μm). This suggests that the vacant hollow was occupied by the primary microcapsule B.

Fig. 2

3.3 Mechanical properties

The mechanical properties of microcapsules A, A-CS, B, B-CS, and microparticles CS were evaluated using a micromanipulation technique that is based on compression of single microcapsules at a given speed

to rupture (Zhang et al., 1999). A typical force *vs.* distance curve is presented in Fig. 3 for all the microcapsules. There was only one peak in this curve for the primary microcapsules A and B, whereas multiple peaks were observed in the curves for the CS particles and the composite microcapsules A-CS and B-CS. The multiple peaks reflect multiple rupture events during compression of the microcapsules. For the composite microcapsules, these multiple peaks might correspond to cracking of the stiff CS shell during the initial breaking, subsequent compression of the debris, and then rupture of the encapsulated primary microcapsules.

Fig. 3

For the microcapsules and microparticles showing multiple peaks, the rupture force corresponding to the first peak was calculated. The deformation at rupture and rupture stress are summarized in Table 1. A large difference in the deformation at rupture, which is defined by the ratio of the displacement at rupture to initial diameter, between microcapsules A (24.9±1.5)% and B (7.5±0.4)% was observed. However, after encapsulation in the CS matrix, the deformations at rupture of composite microcapsules A-CS (25.7±1.0)% and B-CS (26.7±1.9)% were very similar. The nominal rupture stress results gave a similar picture. The average nominal rupture stress results for A and B were 1.30±0.10 and 0.22±0.03 MPa, respectively. Whereas those for A-CS and B-CS were 21.00±2.37 and 21.84±1.43 MPa, respectively. These results suggest that the mechanical properties of the composite microcapsules are dominated by the CS matrix, and are not affected by the type of microcapsule that is encapsulated in the CS. The nominal rupture stress is a reflection of the mechanical strength of a material, and a large increase (16- and 109-fold for A and B, respectively) in the nominal rupture stress from primary microcapsules A and B to composite microcapsules A-CS and B-CS was observed. This indicates that the CS composites can endure greater external force, and in doing so, protect the encapsulated microcapsules from mechanical stress. This increase in the rupture stress of the composite microcapsules is in agreement with a previous report by Leick et al. (2011), who found that the addition of shellac to liquid-filled pectinate capsules increased the strength and stiffness of the capsule wall compared to the pure pectinate capsules. The bare CS microparticles showed lower displacement at rupture (20.9±1.8)% and lower nominal rupture stress (14.1±0.6 MPa) than the composite A-CS and B-CS microcapsules. This indicates that the incorporation of the primary microcapsules A and B enhances the mechanical strength compared with that of CS alone. This result is in agreement with a previous study (White et al., 2001).

Table 1

3.4 Leakage

Oil leakage from microcapsules A, B, A-CS, and B-CS was monitored over 20 d and the release curves are presented in Fig. 4. The microcapsules B had the highest leakage over 20 d (10.3±0.42)%, followed by A (6.8±1.5)%. Composite microcapsules B-CS showed a large reduction in leakage (0.76±0.02)% compared with A and B, and the lowest level of leakage was observed from A-CS

(0.18±0.02)%. However, because of the differences among the average sizes of the microcapsules (A=13.1 μm, B=13.8 μm, A-CS=83.0 μm, and B-CS=84.0 μm), the effect of microcapsule surface area and volume on leakage should be considered.

Fig. 4

Diffusion of a solute molecule from a sphere to a surrounding liquid is described by the following equation (Crank, 1975):

$$\frac{M_t}{M_\infty} = 1 - \frac{6}{\pi^2}\sum_{n=1}^{\infty}\frac{1}{n^2}\exp\left[-\frac{\pi^2 D n^2 t}{a^2}\right], \tag{1}$$

where M_t is the amount of the solute released at time t, M_∞ is the total amount of solute in the microcapsule, D is the diffusivity of the solute in the microcapsule, and a is the radius of the microcapsule. For ratios of M_t/M_∞ less than 40%, the relationship between M_t/M_∞ and $(Dt)^{1/2}/a$ is approximately linear (Ritger & Peppas, 1987) and given by the following equation:

$$\frac{M_t}{M_\infty} = 3\frac{(Dt)^{0.5}}{a}. \tag{2}$$

In the present study, Eq. (2) was applied to evaluate the diffusivity of perfume from the different microcapsules, and it was assumed the leakage mechanism was dominated by Fickian diffusion.

From Eq. (2), M_t/M_∞ *vs.* $t^{1/2}$ was plotted, and the relationship is shown in Fig. 5. D_{eff} can be obtained from the slope of the line. Theoretically, if the microcapsules have a size distribution that is not very narrow, then Eqs. (1) and (2) need to be corrected. However, for small ratios of M_t/M_∞ (<10%) the effect of the size distribution of spheres on the relationship is negligible. Therefore, the mean microcapsule diameter was used to determining D_{eff}.

Fig. 5

The results showed that after taking the diameter into consideration, composite microcapsules A-CS gave the smallest D_{eff} (3.3×10^{-18} m^2/s), followed by B-CS (5.9×10^{-17} m^2/s). By comparison, the values of D_{eff} for microcapsules A and B were 1.4×10^{-16} and 3.8×10^{-16} m^2/s, respectively. The smaller diffusivities for composite microcapsules A-CS and B-CS compared with the primary microcapsules A and B indicate that the flow of core content from the microcapsules to the outside environment is slower for the composite than the primary microcapsules. This proves that the CS matrix effectively reduces leakage of core oil through diffusion inhibition.

4. Conclusions

Composite microcapsules A-CS and B-CS were successfully prepared. The average nominal rupture stresses of the composite microcapsules A-CS and B-CS were 21.0±2.4 and 21.8±1.4 MPa, respectively. The former is approximately 16-fold greater than that of microcapsules A, and the latter was 109-fold greater than that of microcapsules B. Leakage tests showed a 37-fold reduction in leakage after microcapsules A were encapsulated in composite microcapsules (A-CS), and a 14-fold reduction after microcapsules B in composite microcapsules B-CS. After normalizing the sizes of both the microcapsules, composite microcapsules A-CS and B-CS showed much smaller D_{eff} values than microcapsules A and B. This reduction in leakage and enhancement in mechanical strength provides good evidence that CS is an effective carrier that protects the primary microcapsules from rupture. CS provides an additional barrier for diffusion of the encapsulated active ingredients to surrounding aqueous environment.

Because CS slowly dissolves under alkaline conditions (pH>7), these composite microcapsules could be used for double release. For example, instant release of encapsulated A and B microcapsules from the matrix with dissolution of CS, followed by further prolonged release of the core oil by diffusion through the primary microcapsule walls. Furthermore, these composite microcapsules show greater mechanical strength over conventional microcapsules, and they could meet the strength requirements for a wider range of applications.

Acknowledgements

Y. L. was supported by the School of Chemistry, University of Birmingham through the Overseas Research Student Awards Scheme and Procter and Gamble. Some of the equipment used in this research were obtained through Birmingham Science City: Innovative Uses for Advanced Materials in the Modern World (West Midlands Centre for Advanced Materials Project 2), with support from Advantage West Midlands (AWM) and part funded by the European Regional Development Fund (ERDF). We would also like to thank the Engineering and Physical Sciences Research Council (EPSRC) for funding (Grant No. EP/F068395/1).

References

Chauhan, O. P., Raju, P. S., Singh, A., & Bawa, A. S. (2011). Shellac and aloe-gel-based surface coatings for maintaining keeping quality of apple slices. *Food Chemistry, 126*(3), 961-966.

Crank, J. (1975). *The mathematics of diffusion*. Oxford: Clarendon Press.

De Cock, L. J., De Koker, S., De Geest, B. G., Grooten, J., Vervaet, C., & Remon, J. P., et al. (2010). Polymeric multilayer capsules in drug delivery. *Angewandte Chemie International Edition, 49*(39), 6954-6973.

Graf, N., Albertini, F., Petit, T., Reimhult, E., Vörös, J., & Zambelli, T. (2011). Electrochemically

stimulated release from liposomes embedded in a polyelectrolyte multilayer. *Advanced Functional Materials, 21*(9), 1666-1672.

Hamad, S. A., Stoyanov, S. D., & Paunov, V. N. (2012). Triggered cell release from shellac–cell composite microcapsules. *Soft Matter, 8*(18), 5069-5077.

Hamad, S. A., Stoyanov, S. D., & Paunov, V. N. (2013). Triggered release kinetics of living cells from composite microcapsules. *Physical Chemistry Chemical Physics, 15*(7), 2337-2344.

Katagiri, K., Imai, Y., & Koumoto, K. (2011). Viariable on-demand release function of magnetoresponsive hybrid capsules. *Journal of Colloid and Interface Science, 361*(1), 109-114.

Ke, H., Wang, J., Dai, Z., Jin, Y., Qu, E., & Xing, Z., et al. (2011). Gold-nanoshelled microcapsules: A theranostic agent for ultrasound contrast imaging and photothermal therapy. *Angewandte Chemie International Edition, 50*(13), 3017-3021.

Leick, S., Kott, M., Degen, P., Henning, S., Päsler, T., & Suter, D., et al. (2011). Mechanical properties of liquid-filled shellac composite capsules. *Physical Chemistry Chemical Physics, 13*(7), 2765-2773.

Limmatvapirat, S., Limmatvapirat, C., Puttipipatkhachorn, S., Nunthanid, J., Luangtana-anan, M., & Sriamornsak, P. (2008). Modulation of drug release kinetics of shellac-based matrix tablets by in-situ polymerization through annealing process. *European Journal of Pharmaceutics and Biopharmaceutics, 69*(3), 1004-1013.

Long, Y., Vincent, B., York, D., Zhang, Z., & Preece, J. (2010). Organic–inorganic double shell composite microcapsules. *Chemical Communications, 46*(10), 1718-1720.

Long, Y., York, D., Zhang, Z., & Preece, J. (2009). Microcapsules with low content of formaldehyde: preparation and characterization. *Journal of Materials Chemistry, 19*(37), 6882-6887.

Oehme, A., Valotis, A., Krammer, G., Zimmermann, I., & Schreier, P. (2011). Preparation and characterization of shellac-coated anthocyanin pectin beads as dietary colonic delivery system. *Molecular Nutrition & Food Research, 55*(S1), S75-S85.

Pearnchob, N., Siepmann, J., & Bodmeier, R. (2003). Pharmaceutical applications of shellac: Moisture-protective and taste-masking coatings and extended-release matrix tablets. *Drug Development and Industrial Pharmacy, 29*(8), 925-938.

Ravi, V., Siddaramaiah, & Kumar, T.M.P. (2008). Influence of natural polymer coating on novel colon targeting drug delivery system. *Journal of Materials Science: Materials in Medicine, 19*(20), 2131-2136.

Ritger, P. L., & Peppas, N. A. (1987). A simple equation for description of solute release 1. Fickian and non-fickian release from non-swellable devices in the form of slabs spheres cylinders or discs. *Journal of Controlled Release, 5*(1), 23-36.

Singh, A. N., Upadhye, A. B., Mhaskar, V. V., & Dev, S. (1974). Chemistry of Iac resin—VI: Components of soft resin. *Tetrahedron, 30*(7), 867-874.

Skirtach, A. G., Dejugnat, C., Braun, D., Susha, A. S., Rogach, A. L., & Parak, W. J., et al. (2005). The role of metal nanoparticles in remote release of encapsulated materials. *Nano Letters, 5*(7), 1371-1377.

Sukhorukov, G. B., Fery, A., Brumen, M., & Möhwald, H. (2004). Physical chemistry of encapsulation and release. *Physical Chemistry Chemical Physics, 6(*16), 4078-4089.

Upadhye, A. B., Wadia, M. S., Mhaskar, V. V., & Dev, S. (1970). Chemistry of lac resin—IV: Pure lac resin—1: Isolation and quantitative determination of constituent acids. *Tetrahedron, 26*(17), 4177-4187.

White, S. R., Scottos, N. R., Geubelle, P. H., Moore, J. S., Kessler, M. R., & Siram, S. R., et al. (2001). Autonomic healing of polymer composites.. *Nature, 409*(6822), 794-797.

Xue, J., & Zhang. Z. (2008). Preparation and characterization of calcium-shellac spheres as a carrier of carbamide peroxide. *Journal of Microencapsulation, 25*(8), 523-530.

Xue, J., & Zhang, Z. (2009). Physical, structural, and mechanical characterization of calcium–shellac microspheres as a carrier of carbamide peroxide. *Journal of Applied Polymer Science, 113*(3), 1619-1629.

Yow, H. N., & Routh, A. F. (2006). Formation of liquid core-polymer shell microcapsules. *Soft Matter, 2*(10), 940-949.

Zhang, Z., Saunders, R., & Thomas, C. R. (1999). Mechanical strength of single microcapsules determined by a novel micromanipulation technique. *Journal of Microencapsulation, 16*(1), 117-124 .

Zhou, R., Li, Y. F., Yan, L. P., & Xie, J. (2011). Effect of edible coatings on enzymes, cell-membrane integrity, and cell-wall constituents in relation to brittleness and firmness of Huanghua pears (*Pyrus pyrifolia* Nakai, cv. Huanghua) during storage. *Food Chemistry, 124*(2), 569-575.

Table 1 Mechanical properties of microcapsules A, B, A-CS, B-CS, and microparticles CS

Microcapsules or microparticles	Diameter (μm)	Deformation at rupture (%)	Nominal rupture stress (MPa)
A	13.1±1.1	24.9±1.5	1.30±0.10
B	13.8±1.5	7.5±0.4	0.22±0.03
A-CS	83.0±1.7	25.7±1.0	21.00±2.37
B-CS	84.0±1.4	26.7±1.9	21.84±1.43
CS	42.6±1.6	20.9±1.8	14.10±1.60

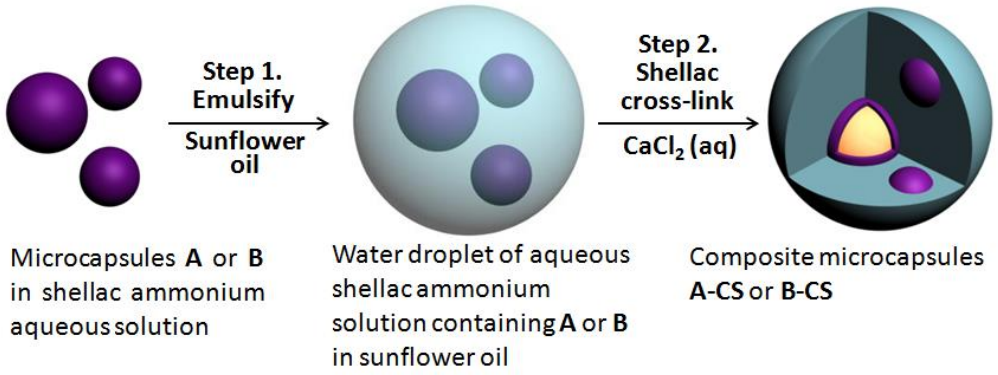

Scheme 1. Schematic representation of formation of the composite microcapsules: Step 1, emulsification of shellac ammonium aqueous solution with melamine formaldehyde microcapsules (A) or $CaCO_3$ nanoparticles stabilized microcapsules (B) in sunflower oil to form water-in-oil emulsion; Step 2, addition of calcium chloride to the emulsion formed in Step 1 to form composite microcapsules A-CS or B-CS with the solidified calcium shellac matrix wall. The cross-section shows the encapsulated primary microcapsules (in purple) and the encapsulated perfume oil (in yellow).

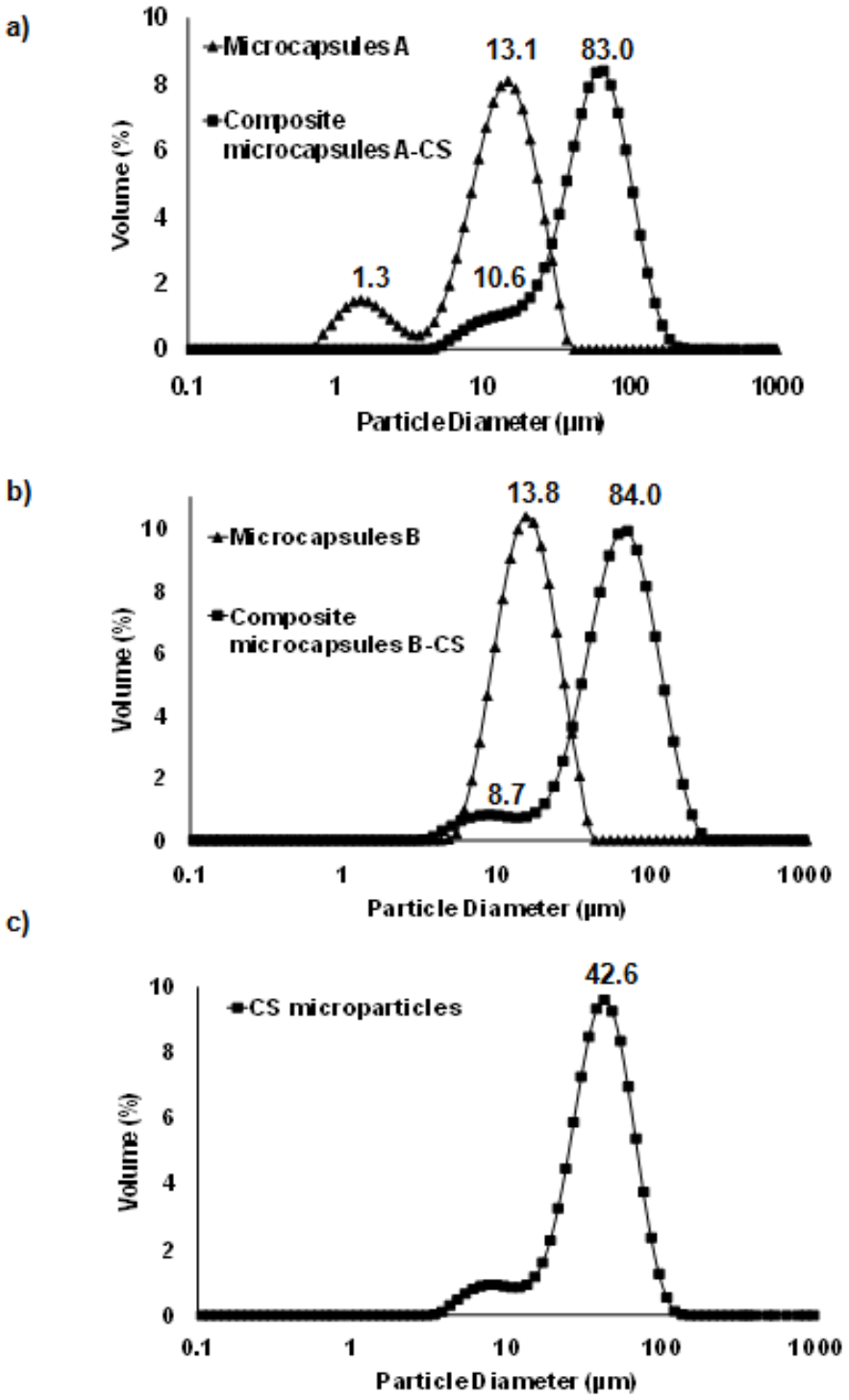

Fig. 1. Average size and size distribution of microcapsules A and B, composite microcapsules A-CS and B-CS, and CS microparticles.

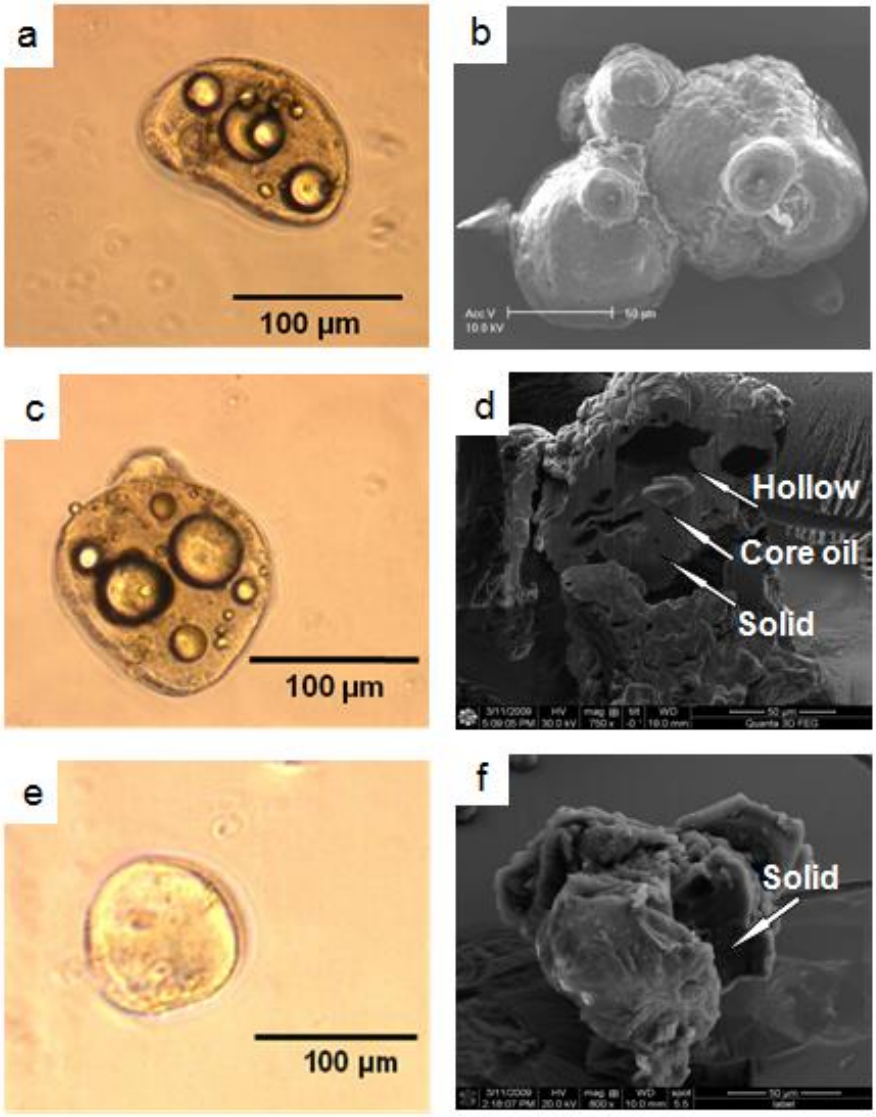

Fig. 2. Optical microscopy and SEM images of the composite microcapsules A-CS ((a) and (b)), B-CS ((c) and (d)) and CS microparticles ((e) and (f)). In images (d) and (f), B-CS and CS were sliced using a focused ion beam technique and observed by SEM.

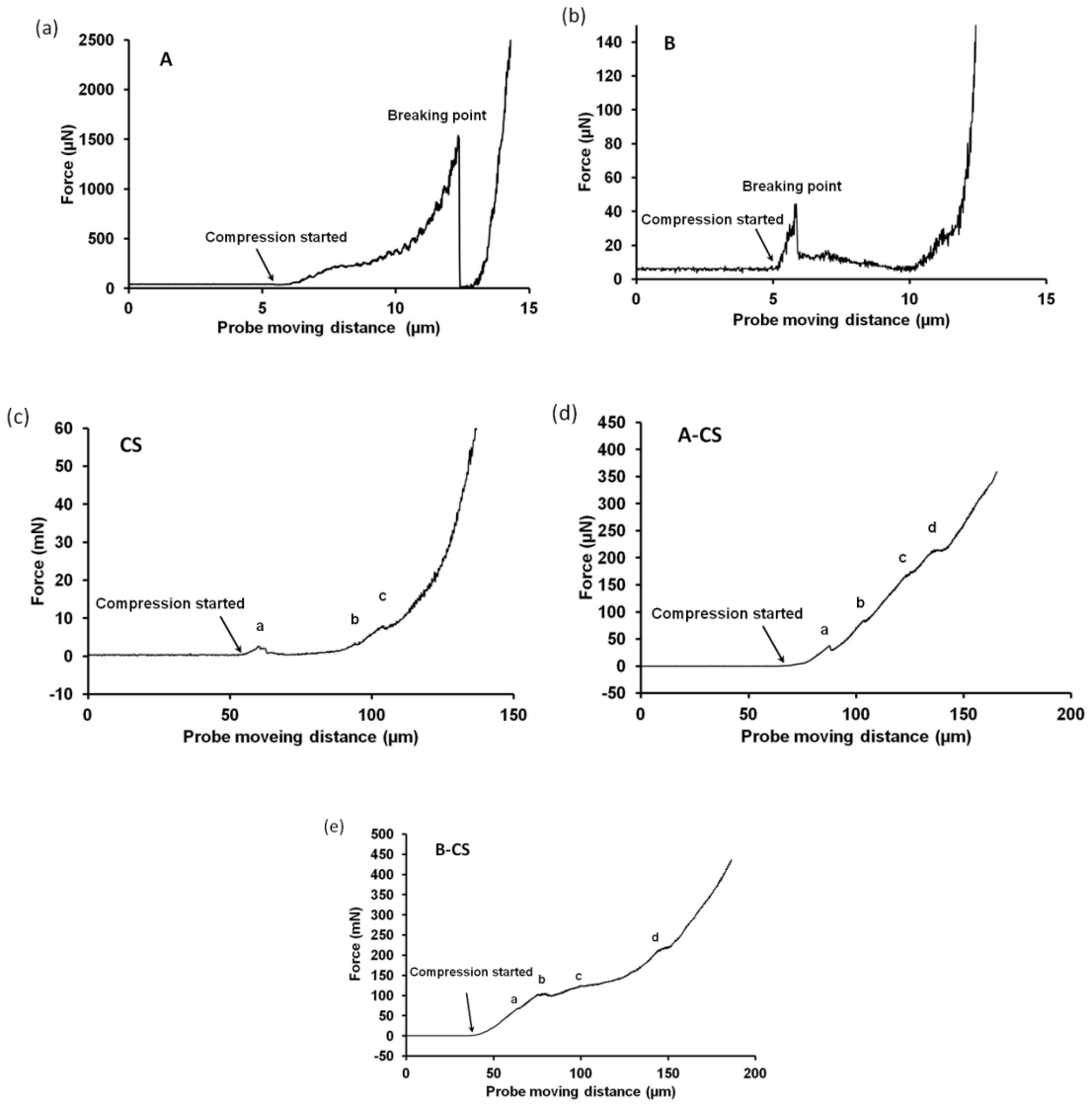

Fig. 3. Typical force *vs.* distance curves for microcapsules. (a), (b) Microcapsules A and B. (c) Calcium shellac microparticles CS, where a–c are the cracking or breakage points. (d) Composite microcapsules A-CS, where a–d are the cracking or breakage points. (e) Composite microcapsules B-CS, where a–d are the cracking or breakage points.

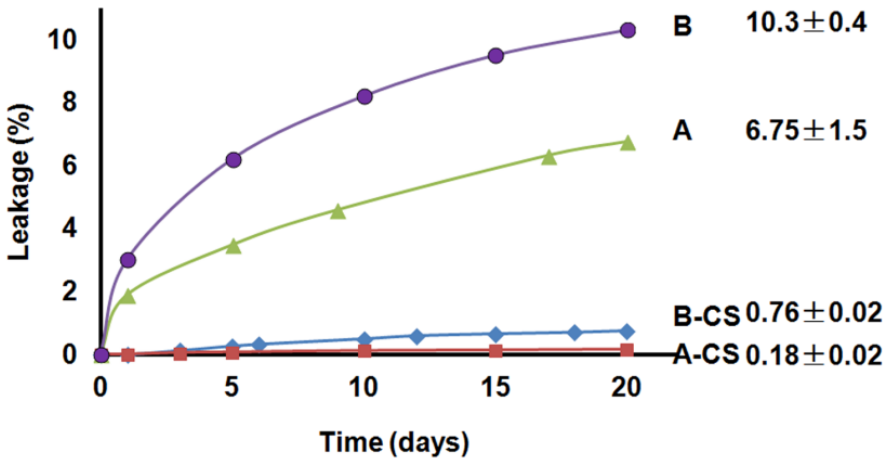

Fig. 4. Leakage profile of microcapsules A, B, A-CS, and B-CS over 20 d. The lines are a guide but not lines of best fit.

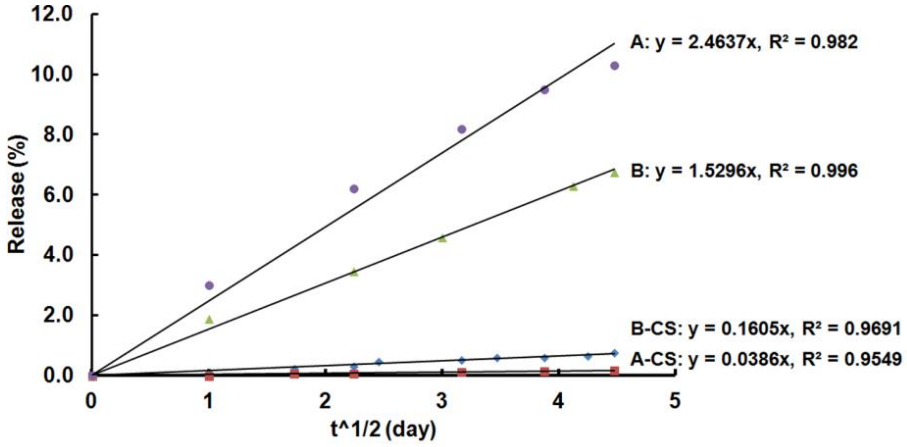

Fig. 5. Linear plots for calculation of D_{eff} for microcapsules A and B, and composite microcapsules A-CS and B-CS.